Journal of Vertebrate Paleontology
Publication details, including instructions for authors and subscription information:
http://www.tandfonline.com/loi/ujvp20

Redescription of Dasypus punctatus Lund, 1840 and considerations on the genus Propraopus Ameghino, 1881 (Xenarthra, Cingulata)

Mariela C. Castro [a] , Ana Maria Ribeiro [b] , Jorge Ferigolo [b] & Max C. Langer [c]

[a] División Paleontología de Vertebrados, Museo de La Plata, Paseo del Bosque s/n, B1900FWA, La Plata, Buenos Aires, Argentina

[b] Seção de Paleontologia, Museu de Ciências Naturais, Fundação Zoobotânica do Rio Grande do Sul, Rua Dr. Salvador França, 1427, Jardim Botânico, 90690-000, Porto Alegre, Rio Grande do Sul, Brazil

[c] Departamento de Biologia, Faculdade de Filosofia, Ciências e Letras de Ribeirão Preto, Universidade de São Paulo, Av. Bandeirantes, 3900, Monte Alegre, 14040-901, Ribeirão Preto, São Paulo, Brazil

To cite this article: Mariela C. Castro , Ana Maria Ribeiro , Jorge Ferigolo & Max C. Langer (2013): Redescription of Dasypus punctatus Lund, 1840 and considerations on the genus Propraopus Ameghino, 1881 (Xenarthra, Cingulata), Journal of Vertebrate Paleontology, 33:2, 434-447

To link to this article: http://dx.doi.org/10.1080/02724634.2013.729961

Journal of Vertebrate Paleontology 33(2):434–447, March 2013

ARTICLE

REDESCRIPTION OF *DASYPUS PUNCTATUS* LUND, 1840 AND CONSIDERATIONS ON THE GENUS *PROPRAOPUS* AMEGHINO, 1881 (XENARTHRA, CINGULATA)

MARIELA C. CASTRO,*,[1] ANA MARIA RIBEIRO,[2] JORGE FERIGOLO,[2] and MAX C. LANGER[3]
[1]División Paleontología de Vertebrados, Museo de La Plata, Paseo del Bosque s/n, B1900FWA, La Plata, Buenos Aires, Argentina, marielaccastro@yahoo.com.br;
[2]Seção de Paleontologia, Museu de Ciências Naturais, Fundação Zoobotânica do Rio Grande do Sul, Rua Dr. Salvador França, 1427, Jardim Botânico, 90690–000, Porto Alegre, Rio Grande do Sul, Brazil, ana.ribeiro@fzb.rs.gov.br, jorge-ferigolo@fzb.rs.gov.br;
[3]Departamento de Biologia, Faculdade de Filosofia, Ciências e Letras de Ribeirão Preto, Universidade de São Paulo, Av. Bandeirantes, 3900, Monte Alegre, 14040-901, Ribeirão Preto, São Paulo, Brazil, mclanger@ffclrp.usp.br

ABSTRACT—The comparative description of the most complete specimen of *Dasypus punctatus* (Xenarthra, Cingulata), from southeastern Brazil, reveals that the species differs from other Dasypodini by the numerous foramina it has in both buckler and movable osteoderms, providing the basis for the lectotype designation. This species was historically allocated to *Propraopus*, but the inclusiveness and monophyly of that genus are uncertain. A new phylogenetic analysis groups *D. punctatus* with the living species of *Dasypus* in a monophyletic clade for the genus, also supporting a *Propraopus* clade composed of *P. sulcatus* and the type species *P. grandis*. The palatal anatomy corroborates previously suggested affinities between *D. kappleri* and *D. punctatus*. On the contrary, the possible synonymy between *P. grandis* and *P. sulcatus* needs further investigation, given that they differed on a single character. As usual in cingulate systematics, characters related to osteoderm ornamentation proved essential to determine the relationships of taxa. However, their use requires careful sampling in order to account for intraspecific variation biases.

INTRODUCTION

Armadillos (Cingulata, Dasypodidae) are the oldest known xenarthrans, dating back to the early Paleogene of Brazil (Scillato-Yané, 1976; Oliveira and Bergqvist, 1998; Bergqvist et al., 2004) and Argentina (Ameghino, 1902; Simpson, 1948; Vizcaíno, 1994; Tejedor et al., 2009; Carlini et al., 2010). The tribe Dasypodini is one of the most basal lineages (Gaudin and Wible, 2006; Delsuc et al., 2012) and includes the genera *Anadasypus* Carlini, Vizcaíno, and Scillato-Yané, 1997 (middle Miocene of Colombia and Ecuador), *Propraopus* Ameghino, 1881 (?Pliocene–Pleistocene of South America), and *Dasypus* Linnaeus, 1758 (Pliocene–Recent) (Carlini et al., 1997). The latter is the most widespread living genus of Xenarthra, ranging approximately from 40°N to 40°S in the American continent (Wetzel, 1985; Aguiar and da Fonseca, 2008), and also the most taxonomically diverse, with seven living species (Wilson and Reeder, 2005). McKenna and Bell (1997) included *Dasypodon* Castellanos, 1925 (Pleistocene of Bolivia) within Dasypodini, but it likely pertains to Euphractinae, as pointed out by Marshall and Sempere (1991). Recent phylogenetic studies (Pessôa et al., 2008) suggested that the cingulate *Eocoleophorus* Oliveira, Ribeiro, and Bergqvist, 1997 (Oligocene of Brazil), also represents a Dasypodini, but this is still to be confirmed (Carlini and Scillato-Yané, 1999; Ciancio, 2010).

In his pioneering paleontological studies in the karst of Lagoa Santa, Minas Gerais, Brazil, Peter Wilhelm Lund (1840, 1842) named two fossil species of *Dasypus*, both based on numerous osteoderms, as well as cranial and postcranial fragments, subsequently figured and described in detail by Winge (1915). According to the latter author, apart from differences in size and proportions of corresponding elements, *Dasypus punctatus* Lund, 1840 and *D. sulcatus* Lund, 1842 differ from *D. novemcinctus* based mainly on osteoderm features.

The type species of *Propraopus* Ameghino, 1881 (*P. grandis*) was established based on carapace fragments from the Pleistocene of Luján, Buenos Aires Province, Argentina. That author did not have the opportunity to compare the material, which is presently lost (Scillato-Yané, 1982), with those remains described by Lund (1840, 1842). Later, Hoffstetter (1952, 1958) allocated *Dasypus magnus* Wolf, 1875 (Pleistocene of Ecuador), *Dasypus bellus* Simpson, 1929 (Pleistocene of U.S.A.), *D. punctatus*, and *D. sulcatus* within *Propraopus*, an ascription commonly accepted since, except for *D. bellus*. Concerning this matter, in this paper we primarily cite the generic assignation adopted by the researchers we mention; the taxonomic and nomenclatural implications of our study are discussed below.

Previous authors (Paula-Couto, 1979; Scillato-Yané, 1982) questioned the uniqueness of *P. magnus*, *P. grandis*, and *P. sulcatus*, and some (Hoffstetter, 1952; Paula-Couto, 1982) suggested that the former two might represent junior synonyms of *P. sulcatus*. Also, *Propraopus* sensu Hoffstetter (1952, 1958) was found to be paraphyletic by Pessôa et al. (2008). Rincón et al. (2008) recognized similarities between the living *D. kappleri* and the extinct *D. bellus*, *Propraopus punctatus*, and *P. sulcatus*, recommending further comparisons to define their possible placement in a separate genus or subgenus.

Fossils attributed to *Propraopus* are also known from the Pleistocene (Ensenadan–Lujanian SALMA) of Argentina (*P. grandis*; Cione and Tonni, 2005), Bolivia (*P.* cf. *grandis* or *P.* cf. *sulcatus*; Paula-Couto, 1979; Marshall et al., 1984), Venezuela (*P. sulcatus*; Rincón et al., 2008), and Uruguay (*P.* cf. *sulcatus*; Ubilla and Perea, 1999). In the late Pleistocene of Brazil, *P. sulcatus* or *P.* cf. *sulcatus* were recorded in the northeastern, central, and southernmost parts of the country (Faure et al., 1999; Cartelle and Hirooka, 2005; Oliveira and Pereira, 2009), whereas specimens from southeast Brazil (Paula-Couto, 1973, 1980, 1982) were attributed

---

*Corresponding author.

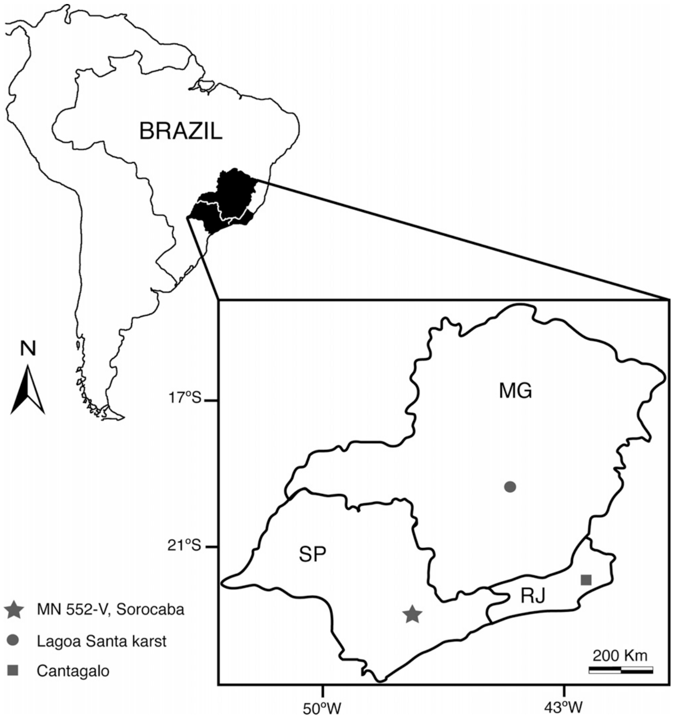

FIGURE 1. Geographic location of fossil sites that yielded *Dasypus punctatus.* **Abbreviations**: **MG**, Minas Gerais; **RJ**, Rio de Janeiro; **SP**, São Paulo.

to *P. punctatus*. There is also a possible occurrence (cf. *Propraopus*) in the Amazon (Paula-Couto, 1983).

Here we redescribe a well-preserved specimen previously referred to *Propraopus punctatus* (Paula-Couto, 1973) from southeastern Brazil, and present a phylogenetic study that supports the allocation of that species to the genus *Dasypus*. Paula-Couto (1973) reported that those fossil remains were collected during the 1960s from a cave named 'Gruta de Itaporanga,' located in the municipality of Sorocaba, São Paulo, Brazil (Fig. 1). Unfortunately, we found no additional geographical information or further mention of the site in the literature.

A late Pleistocene–early Holocene age has been proposed for mammal-bearing Brazilian karst deposits (Cartelle, 1999; but see Auler et al., 2006). This assignment is based both on the comparison with well-known Argentinean local faunas (Marshall et al., 1984) and on several radiometric dates (Faure et al., 1999; Neves and Piló, 2003; Hubbe et al., 2007, 2009).

Institutional Abbreviations—**CC**, Museu de Arqueológico e Paleontológico Casa Dom Aquino, Cuiabá, Brazil; **IGM**, INGEOMINAS, Bogotá, Colombia; **MACN**, Museo Argentino de Ciencias Naturales 'Bernardino Rivadavia', Buenos Aires, Argentina; **MCN-MA**, Coleção de Mastozoologia, Museu de Ciências Naturais, Fundação Zoobotânica do Rio Grande do Sul, Porto Alegre, Brazil; **MCN-PV**, Coleção de Palentologia de Vertebrados, Museu de Ciências Naturais, Fundação Zoobotânica do Rio Grande do Sul, Porto Alegre, Brazil; **MLP**, Museo de La Plata, La Plata, Argentina; **MN**, Museu Nacional, Rio de Janeiro, Brazil; **MZUSP**, Museu de Zoologia da Universidade de São Paulo, São Paulo, Brazil; **YPM-PU**, Princeton University Collection at Yale Peabody Museum of Natural History, New Haven, Connecticut, U.S.A.; **ZMK**, Zoologisk Museum, Copenhagen, Denmark.

Other Abbreviations—**CI**, consistency index; **RI**, retention index; **SALMA**, South American Land Mammal Age.

SYSTEMATIC PALEONTOLOGY

XENARTHRA Cope, 1889
CINGULATA Illiger, 1811
DASYPODIDAE Gray, 1821
DASYPODINAE Gray, 1821
DASYPODINI Gray, 1821
DASYPUS PUNCTATUS Lund, 1840
(Figs. 2–7)

Lectotype (Designated Herein)—ZMK 1/1845:13767, a buckler osteoderm (Fig. 2A).

Paralectotypes—Other former syntypes.

Type Locality—Lapa dos Tatus, Lagoa Santa karst, Minas Gerais, Brazil (approximately 19°31′35″S and 44°00′20″W).

Referred Specimens—MN 552-V: carapace fragments, isolated osteoderms, partial skull and mandible, and postcranial elements including atlas, axis, and three posterior cervical vertebrae, four partial thoracic vertebrae, four posterior-most lumbar vertebrae, two anterior-most sacral vertebrae, partial left scapula, left humerus, left ulna, partial left manus, rib fragments, right ilium, distal portion of right femur, and right patella (specimens described herein); MCN-PV 009: carapace fragment; MCN-PV 014: isolated osteoderm. Specimens CC 897 and CC 900 (a movable and a buckler osteoderm, respectively) from Rosário do Oeste, Mato Grosso, were mistakenly referred as *P. punctatus* by Cartelle and Hirooka (2005), but are instead attributed to *P. sulcatus*, because it has fewer foramina. The specimens from the Lund collection (ZMK) were not analyzed first hand and, except for the lectotype (see Acknowledgments), are not included in this list.

Distribution—Late Pleistocene–early Holocene of southeastern Brazil: Lagoa Santa region, Minas Gerais; Sorocaba municipality, São Paulo; Cantagalo municipality, Rio de Janeiro (Fig. 1).

Diagnosis—*Dasypus punctatus* has a unique combination of carapace features, including most buckler osteoderms with 10 foramina in the principal sulcus (ranging from six to sixteen); most movable osteoderms with 12 foramina in the principal sulcus/sulci (ranging from 9 to 18); and most movable osteoderms with five piliferous foramina in the posterior border (ranging from four to seven) (Fig. 2). As a whole, this indicates that osteoderms of *D. punctatus* have a greater number of foramina than other Dasypodini, a condition here interpreted as autapomorphic for the taxon. A comparison of these features in 10 related taxa is provided in Tables 1 and 2.

DESCRIPTION AND COMPARISONS

Given that the skeletal remains from MN 552-V do not include duplicated elements and share equivalent size and preservation, it is assumed that they belong to a single individual. Comparisons were based mostly on direct observations of specimens (Appendix 1), as well as on published accounts. Anatomical terminology follows the treatise of Wible and Gaudin (2004) for the cranial osteology, whereas for the postcranial elements we adopted the most usual forms from the current literature. Due to the historical importance of the specimen, no additional preparation was attempted, especially in delicate parts of the skull (e.g., the right orbital region, jugal bone, and medial surface of the dentary). Entire carapaces were sampled for *P. grandis* (MLP 69-IX-9-9) and living species of *Dasypus*. Their variation was compared with carapace fragments of MN 552-V and *P. sulcatus* in order to recognize differences related to position.

Osteoderms

The osteoderms of *Dasypus punctatus* have the typical morphology of the genus (Vizcaíno, 1994; Hill, 2006; Vickaryous and Hall, 2006; Krmpotic et al., 2009). The internal surface of both buckler and movable elements are relatively smooth and bear

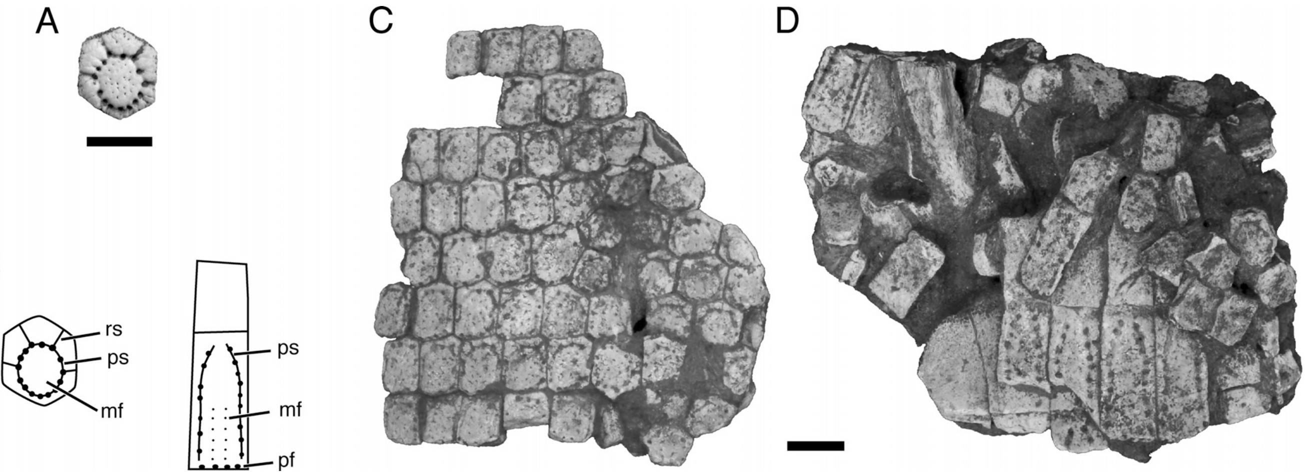

FIGURE 2. Osteoderms of *Dasypus punctatus* in external view. **A**, lectotype designated herein, a buckler osteoderm, ZMK 1/1845:13767; **B**, line drawing of the major structures mentioned in the text to buckler and movable osteoderms; **C**, fragment of the scapular buckler, MN 552-V; **D**, movable osteoderms, MN 552-V. **Abbreviations**: **mf**, main figure; **pf**, piliferous fomanina; **ps**, principal sulcus; **rs**, radial sulcus. Scale bars equal 10 mm.

one to three irregularly distributed foramina. In order to estimate variation, the ornamented external surface of all complete osteoderms of *Dasypus punctatus* was analyzed (Fig. 2). Most buckler osteoderms are hexagonal and bear 10 foramina in the principal sulcus, although there are four- to seven-sided elements, with 6–16 foramina. The main figure is subcircular to polygonal, smoothly convex or nearly flat, and displaced toward the posterior margin of the osteoderm. There are numerous small neurovascular perforations randomly distributed throughout the main figure. The radial sulci form three to five peripheral figures, eventually more convex than the main figure, clustered toward the anterior and lateral borders. The depth of the sulci varies among osteoderms, and a foramen usually perforates the intersection between the principal sulcus and each radial sulcus. Relative to the scapular osteoderms, the pelvic elements are larger and bear more foramina. In both bucklers, osteoderms located closer to the movable bands are larger. The anterior portion of movable osteoderms is separated from the posterior ornamented portion by an unwrinkled transverse depression, which may bear small foramina. The ornamented portion has two principal sulci that diverge toward the edge. These are anteriorly connected in some osteoderms, forming an inverted ‘U’- or ‘V’-shaped sulcus. Most elements have a total of 12 foramina in the principal sulcus/sulci, although the number may range from 9–18. In addition, small neurovascular perforations are distributed along two longitudinal lines on the triangular main figure. The posterior border of most elements has five piliferous foramina, with a range from four to seven.

Dasypus punctatus differs from other Dasypodini by having a greater number of foramina in the principal sulci of buckler (Table 1) and movable osteoderms (Table 2). The arrangement of foramina in the principal sulcus of buckler osteoderms also distinguishes *D. punctatus* from *P. grandis* and *P. sulcatus*, which have these foramina restricted to the anterior half of the osteoderms. The carapace of *Stegotherium tauberi* is very distinct from that of Dasypodini, precluding most comparisons between their osteoderms (see Phylogenetic Analysis below). Because size may greatly vary according to the position in the carapace, this criterion was not adopted to differentiate taxa, but is illustrated for the buckler osteoderms of *D. punctatus*, *D. novemcinctus*, *P. grandis*, and *A. hondanus* in Table 3.

Skull

The preserved external surface of the cranium includes maxilla, nasal, premaxilla, lacrimal, jugal (latter four bones only on left side), palatine, ethmoid, alisphenoid (both only on the right

TABLE 1. Comparison of buckler osteoderms of *Dasypus punctatus* with other Dasypodini.

Taxon	Foramina in the principal sulcus, minimum–maximum (most frequent occurrence)	Foramen in at least one intersection between principal and radial sulci	Distribution of foramina in the principal sulcus
D. punctatus	6–16 (10)	Present	All over
D. novemcinctus	2–7 (4)	Present/absent	All over
D. septemcinctus	2–4 (3)	Present/absent	Restricted to the cranial half
D. sabanicola (Rincón et al., 2008)	1–5	Present	All over
D. hybridus	4–9 (6)	Present	All over
D. kappleri	3–9	Present	All over
D. yepesi	3–8 (4)	Present	All over
D. bellus (Downing and White, 1995; Hill, 2006)	3–5	Present	All over
Propraopus grandis	2–5 (3)	Absent	Restricted to the cranial half
P. sulcatus (Winge, 1915:pl. V.3,4)	2–4 (3)	Absent	Restricted to the cranial half
Anadasypus	2–5 (3)	Present	Restricted to the cranial half*

*The principal sulcus is roughly semicircular and entirely restricted to the cranial half of the osteoderm.

TABLE 2. Comparison of movable osteoderms of *Dasypus punctatus* with other Dasypodini.

Taxon	Principal sulci anteriorly connected	Foramina in the principal sulci, minimum–maximum (most frequent occurrence)	Piliferous foramina in the posterior border, minimum–maximum (most frequent occurrence)
D. punctatus	Rarely present	9–18 (12)	4–7 (5)
D. novemcinctus	Commonly present (80%)	7–13 (10)	1–4 (4)
D. septemcinctus	Absent	3–5	1–4
D. sabanicola (Rincón et al., 2008)	?	2–7	3–4
D. hybridus	Rarely present	5–12 (7)	1–4 (2)
D. kappleri	Present/absent	6–8	2–4
D. yepesi	Present/absent	6–9 (7)	1–3
D. bellus (Hill, 2006:fig. 9)	Absent	6	2
Propraopus grandis	Absent	2–4	1–3
P. sulcatus (Winge, 1915:pl. V.3,4)	Absent	5–8	2
Anadasypus	Absent	5–7 (6)	0–2 (1)

side), frontal, squamosal, pterygoid, basisphenoid, and basioccipital bones. The left dentary and upper and lower dentition are partially preserved (Figs. 3–5). Skull measurements of MN 552-V compared with *D. novemcinctus* (MCN-MA 2788) and *P. grandis* (MACN 17989) are given in Table 4. For more complete ranges of measurements on living *Dasypus*, see Wetzel and Mondolfi (1979) and Wetzel (1985).

Facial and Palatal Regions—The anterior-most portion of the skull is preserved as an internal cast (Fig. 3). In dorsal view, the lateral borders of the facial region are concave. The preserved posterior half of the nasal is elongated and narrow. The contact with the maxillary is straight and roughly parallel to the internasal suture, whereas the posterior border contacts the frontal. The broken external surface permits the observation of convoluted turbinals on the right side (Fig. 4). The palate is generally flat, with no crests. The premaxilla is represented only as prong extending over the palatal portion of the left maxilla. The maxillae have sizeable facial and palatal exposures, proportionally larger than those of *D. novemcinctus*. For descriptive purposes, the maxilla is divided into three areas: facial, palatine, and zygomatic processes. From anterior to posterior, the medial border of the facial process contacts the nasal, frontal, and lacrimal. In dorsal view, a convex maxillary process extending over the frontal is unique to this specimen. The longitudinal maxillary crest occupies the posterior half of the facial process and is continuous with the lacrimal crest, which is weaker and more dorsally placed in relation to *D. novemcinctus*. The lateral flaring of the maxillary crest contributes to the triangular outline of the rostrum in dorsal and ventral views. The infraorbital canal extends through the posteroventral portion of the maxilla. Its anterior aperture (infraorbital foramen) is continuous with a subtle sulcus (buccinator fossa) at the level of the seventh alveolus (Fig. 5), and the posterior opening (maxillary foramen) is apparently located at the suture with the ethmoid. The palatine process of the maxillae has numerous small vascular foramina, as in *D. novemcinctus* and *D. kappleri*. All eight dental alveoli are preserved in the left maxilla (the dentition is described in a separate section below). Their dimension increases throughout the seven anterior alveoli, and the outer contour is rectangular, except for the circular posterior-most alveolus. Only a small portion of the zygomatic process is preserved, forming the anterior root of the zygoma together with the zygomatic process of the lacrimal, and probably also with the zygomatic process of the jugal, but the latter bone is not preserved in position (Fig. 5). The palatines correspond to more than one-third of the hard palate (Fig. 3B) and are proportionally larger than in other taxa. There are few vascular foramina, all concentrated close to the suture with the palatine process of the maxilla. The posterior border meets the pterygoid at an irregular suture, and both bones form the bell-shaped internal nasal aperture, which is long and broad as in *P. grandis*, and differs from the long and narrow condition of *Stegotherium* and *D. hybridus*. In *D. novemcinctus* it is short and broad, whereas it is almost straight in *D. kappleri*. The orbital exposure of the palatine is very slender, as in modern *Dasypus*. In lateral view, it meets the maxilla, ethmoid, and alisphenoid (sutures partially covered by sediment). The pterygoid is thin and has a broader dorsally projected posterior half. It meets the alisphenoid laterally and the basisphenoid medially. As in other Dasypodini, the palatal process of the pterygoids forms the posterior-most portion of the hard palate, an unusual feature not found in other armadillos (Fig. 3B).

Orbital Region—Despite lacking a tip near the suture with the jugal, the lacrimal is proportionally larger than that of other dasypodine taxa (Fig. 5). Its facial process is roughly triangular, contacting the frontal dorsomedially and the maxilla anteroventrally. Continuous with the maxillary crest, the lacrimal crest extends to the root of the zygoma. A posterior sulcus emerges from the lacrimal foramen; in *P. grandis* the sulcus is absent and the foramen is more posterior. The small orbital process is slightly concave, lying at an approximately 90° angle to the facial

TABLE 3. Measurements (mm) of buckler osteoderms of *Dasypus punctatus*, *D. novemcinctus*, *Propraopus grandis*, and *Anadasypus hondanus*.

Taxon	Length	Width	Thickness
D. punctatus	8.3–10.9	6.3–9.3	3.3–3.9
D. novemcinctus	4.2–6.7	4.0–6.4	1.2–1.9
P. grandis	9.6–19.3	4.8–18.6	4.1–5.5
A. hondanus	6.5–9.5	6.0–7.5	3.1–4.2

TABLE 4. Cranial measurements (mm) of *Dasypus punctatus* compared with those of *D. novemcinctus* and *Propraopus grandis*.

Dimension	*D. punctatus*	*D. novemcinctus*	*P. grandis*
Greatest skull length	119*	93.5	209*
Rostral length	81*	59.6	132*
Length of upper tooth row	30.9	22.8	50.4
Palatal length at mid-level	75*	62.3	105*
Interorbital width	33.4	22.8	43.7
Width of glenoid articulation	5.3	6.0	11.8
Width of sphenoccipital suture	13.4	11.1	22.8
Greatest dentary length	112*	83.2	171*

*Measurements estimated by assuming that incomplete skull/dentary were proportional to those of *D. novemcinctus* of similar inferred age.

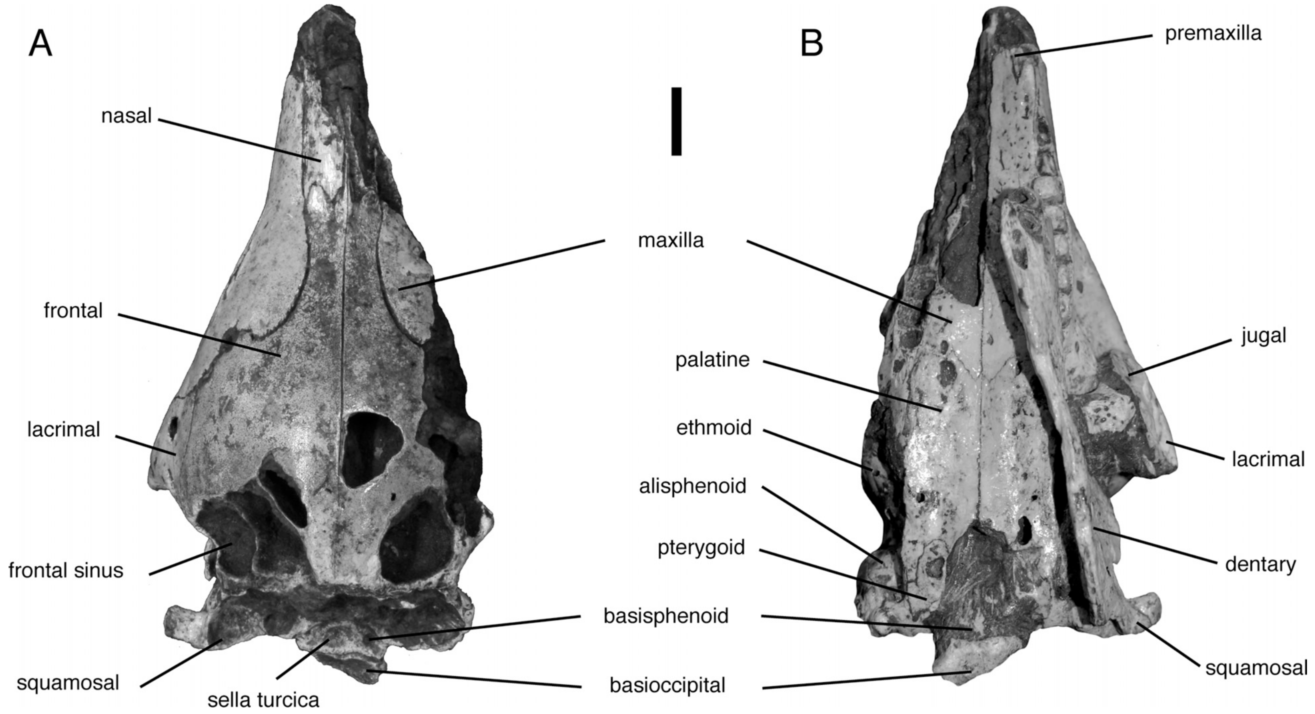

FIGURE 3. Skull of *Dasypus punctatus*, MN 552-V. **A**, in dorsal view; **B**, in ventral view. Scale bar equals 10 mm.

process. Damage to the external surface has exposed the lacrimomaxillary sinus, which is as large as that of *D. novemcinctus* (see Macrini, 2005). Adhered to sediment on the left side of the skull (Fig. 5), the jugal contacted the zygomatic processes of the maxilla and lacrimal anteriorly, and the squamosal posteriorly, forming the lateral limit of the orbit, as in other dasypodids. The anterior surface bears a rounded depression, bordered dorsally by a ridge that is continuous with the lacrimal crest. The orbital exposure of the ethmoid is located on the ventral surface of the orbital wall, and broken parts reveal its extreme thinness (Fig. 4). Only the frontal and the alisphenoid contacts are preserved, and the posterior border forms the medial wall of the sphenorbital fissure. Ethmoturbinals are represented on the right side of the skull as an internal cast. Observed in *Stegotherium tauberi* González and Scillato-Yané, 2008 (see Scott, 1903–1904), *P. grandis*, MN 552-V, and extant *Dasypus*, the large orbital exposure of ethmoid represents a synapomorphy of Dasypodinae (Gaudin and Wible, 2006).

Neurocranial and Basicranial Regions—The paired frontals contribute to both skull roof and orbitotemporal region (Figs. 3–5). The dorsal portion of each frontal is composed of an anteromedial projection and a convex posterior portion. This anteromedial projection, proportionally longer than that of *D. novemcinctus*, extends over the nasal as two V-shaped apophyses. Fragmentation reveals asymmetrically distributed frontal sinuses; posterior to those, the skull is broken at the frontoparietal contact (Fig. 3A). Forming an approximately 90° angle with the skull roof, the orbitotemporal part of the frontal contacts the ethmoid, sphenoid complex (alisphenoid), and squamosal (Figs. 4, 5). On the right side, the ventral portion shows two ethmoidal

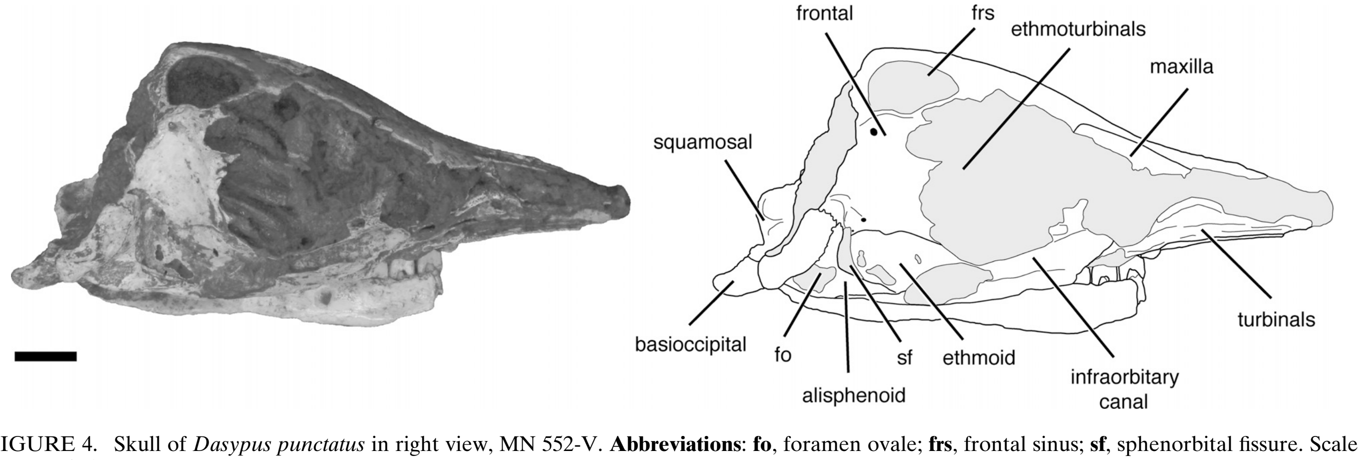

FIGURE 4. Skull of *Dasypus punctatus* in right view, MN 552-V. **Abbreviations**: **fo**, foramen ovale; **frs**, frontal sinus; **sf**, sphenorbital fissure. Scale bar equals 10 mm.

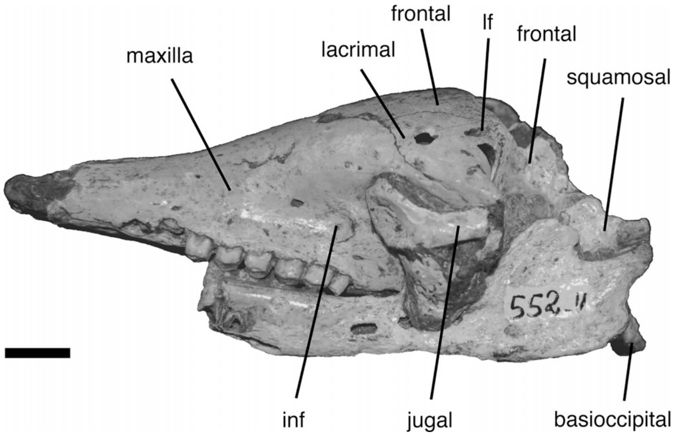

FIGURE 5. Skull of *Dasypus punctatus* in left view, MN 552-V. **Abbreviations**: **inf**, infraorbital foramen; **lf**, lacrimal foramen. Scale bar equals 10 mm.

foramina, and a broken foramen in a posterodorsal position. In *Euphractus sexcinctus*, Wible and Gaudin (2004) identified a similar structure as the anterior opening of the orbitotemporal canal. Another foramen pierces the dorsal-most preserved tip of the right frontal, in a position where three or four foramina are present in *E. sexcinctus* (Wible and Gaudin, 2004). Only small anteroventral portions of both squamosals represent the temporal complex. Contacts with the frontal and alisphenoid can be observed on the right side (Fig. 4). The glenoid articulation is roughly flat, almost parallel to the palate (Fig. 5), as in other Dasypodini. It lacks the posterior part, which in *P. grandis* and modern *Dasypus* has a ventrally projecting postglenoid process. The external surface of the sphenoid complex is represented by partial right alisphenoid and basisphenoid (Fig. 4); the orbitosphenoid is largely covered by sediments. The nearly triangular alisphenoid contacts the squamosal posterodorsally, the lateral border of palatine and pterygoid ventrally, and the frontal anterodorsally. The sphenorbital fissure, foramen ovale, and transverse canal foramen are filled by sediment, precluding their observation. The former shares a common fossa with the optic foramen in *Dasypus* and *Stegotherium* (Gaudin and Wible, 2006). A foramen rotundum was not identified and, as in other Dasypodidae except for *Stegotherium* (Gaudin and Wible, 2006), it is probably confluent to the sphenorbital fissure (Hoffstetter, 1958; Guth, 1961), through which pass the oculomotor, trochlear, ophthalmic, maxillary, and abducens nerves, accompanying veins, and a branch of the maxillary artery (Paula-Couto, 1979; Wible and Gaudin, 2004). A suture between alisphenoid and basisphenoid cannot be distinguished, probably because of an early fusion, as occurs in *E. sexcinctus* (Ferigolo, 1981). Partial absence of the skull roof exposes in the basisphenoid a well-preserved sella turcica (Fig. 3A). An anterior portion of the basioccipital represents the occipital complex. The internal surface is concave, whereas the external is flat, except for a crest that extends along the suture with the basisphenoid, corroborating that it belongs to a young individual. The medial posterior tip corresponds to the odontoid notch of the foramen magnum.

Dentary—Sediment attaches the partial left dentary to the skull (Figs. 3–5). The anterior portion of the body is missing in front of the presumed fifth tooth, and an elongated mandibular foramen is present posterior to the eighth. The alveolar margin is transversely wider than the ventral border, which is slightly convex in lateral view. The thinner ramus is at an obtuse angle to the body. The coronoid process lacks the dorsoposterior tip, and the condylar process widens toward the rectangular and flat articular surface; the two processes are separated by a shallow incisure. The angular process is rounded. Broken surfaces reveal the interalveolar septae between the permanent teeth, as well as the mandibular canal, where the mandibular nerve and corresponding vessels pass. In relation to *D. novemcinctus*, the dentary of MN 552-V is more robust, with a wider coronoid process. Winge (1915) described the dentaries of *D. punctatus* and *D. novemcinctus* as similar, except for the blunter angular process in the former, an observation corroborated by MN 552-V. The same condition is present in *D. kappleri*, *D. septemcinctus*, and *P. grandis* (although the angular process is extremely reduced in the latter), whereas it is sharp in *D. hybridus* and *D. novemcinctus*. The length of the dentary of this specimen, *D. novemcinctus* (MCN-MA 2788), and *P. grandis* (MACN 17989) are compared in Table 4.

Dentition—The specimen was replacing the dental series when it died. It preserves all eight loci on the left maxilla and the posterior four loci on the partial dentary (Figs. 3–5). Although there are some variations on tooth counts in *Dasypus* (Gaudin and Wible, 2006; Ciancio et al., 2012), we assume that the specimen had the typical 8/8 condition. In the upper row, the two anterior-most deciduous teeth are absent and the erupting permanent molariforms are exposed. The remaining maxillary and dentary alveoli bear completely erupted deciduous teeth, except for the posterior-most (Mf8/mf8), which have no precedent (Martin, 1916), and are smaller, with a circular cross-section. Deciduous teeth are prismatic, with rectangular cross-sections. The occlusal relief of DMf3–DMf7 has less worn labial and lingual borders, whereas dmf5–dmf7 have just lingual elevation. True cusps are present only in the non-erupted permanent teeth: Mf1 exhibits a single cusp and Mf2 has a labial and a lingual cusp. Exposed at broken dentary surfaces, mf5 and mf6 are euhypsodont, with a subtle distinction between intra- and extra-alveolar portions. The occlusion pattern is alternate, as in other Dasypodinae.

Postcranium

In general, the postcranial anatomy of *D. punctatus* is very similar to that of extant *Dasypus* and *P. grandis,* indicating that postcranial skeletal morphology is very conservative in the tribe. The few differences recognized are mentioned below.

Cervical Vertebrae—An atlas, partial axis, and fragments of the three next vertebrae are preserved together (Fig. 6A, B). The articular facets for the occipital condyles occupy the whole lateral extension of the atlas, which is more massive than that of *D. novemcinctus*. The neural canal is nearly circular, and the vertebroarterial canal pierces the dorsolateral margins of the neural arch. The foramen for the first spinal nerve opens on the lateral atlantal surface, and meets the vertebroarterial canal internally. Aliform transverse processes project posteriorly and dorsally. The dorsal apophysis for articulation of the neural spine of the axis is abraded. Articular facets for the axis are elliptical and slightly concave. Fusion between the epiphyses indicates that the axis (C2) and the third (C3) and fourth (C4) cervical vertebrae co-ossify into a single element, the mesocervical bone, as in *Stegotherium tauberi* (Scott, 1903–1904), *P. grandis*, and living *Dasypus* (see Galliari et al., 2010, for other vertebral fusions in armadillos). In the axis, the rounded apertures of the vertebroarterial canal are dorsal to the elongated articular facets for the atlas. The odontoid process is dorsally angled, and a convex facet on its ventral border articulates with the neural canal of the atlas. A circular foramen for the second spinal nerve pierces the lateral arch of the axis. The neural spine occupies the whole length of the vertebra and, although fragmented, it certainly overlapped portions of the more posterior cervical vertebra. As in other cingulates, cervical vertebrae C3–C5 have laterally expanded centra. The posterior epiphysis of C4 and the anterior of C5 are not fused to one another or to their respective centra, and sediment fills the

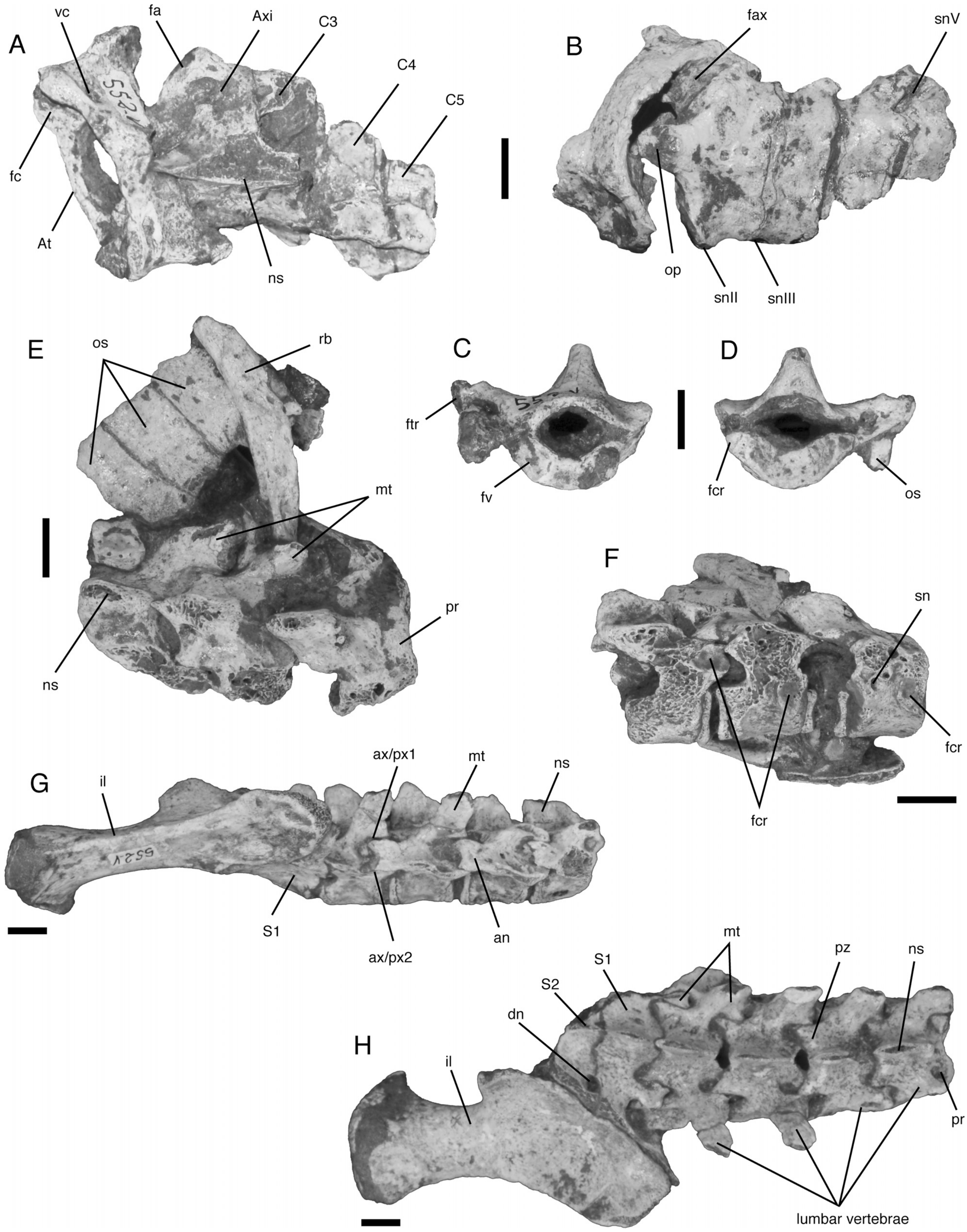
A
vc
fa
Axi
C3
C4
C5
fc
At
ns
B
fax
snV
op
snII
snIII
E
os
rb
mt
ns
pr
C
ftr
fv
D
fcr
os
F
sn
fcr
fcr
G
il
ax/px1
mt
ns
S1
ax/px2
an
H
S1
S2
dn
mt
pz
ns
il
pr
lumbar vertebrae

space previously occupied by the intervertebral disc. Both vertebrae also articulate by their transverse processes, a feature observed in other armadillos as well (Castro and Ferigolo, 2010). Laterally, foramina for emergence of the third to fifth spinal nerves lie between the pedicels of the axis/C3, C3/C4, and C4/C5.

Thoracic Vertebrae and Ribs—Four thoracic vertebrae are partially preserved (Fig. 6C–F). Their centra are narrower transversely and taller dorsoventrally than in the cervical series, and the epiphyses are incompletely fused. The nearly complete isolated vertebra has a massive neural spine. The anterior epiphysis of the centrum bears a pair of rounded lateral facets that articulate to the preceding vertebra, in addition to the broad median attachment, as in other Dasypodidae (Castro and Ferigolo, 2010). The posterior epiphysis of the centrum has lateral facets for the capitulum of the rib. Facets for the tuberculum are lateral to the robust transverse process, which is at an approximately 90° angle to the neural spine. Pre- and postzygapophyses were not preserved. Comparison with other Dasypodini suggests that it is the fifth thoracic element. The other three thoracic vertebrae are articulated and associated with partial ribs and osteoderms. Their morphology indicates that they are posterior to the isolated element, and probably represent the seventh to ninth thoracic vertebrae. Prezygapophyses occupy nearly the entire dorsoanterior border of the neural arch, and the postzygapophyses are exposed in the anterior-most vertebra. In this, and also in the posterior-most vertebra, a circular foramen for spinal nerve emergence pierces the ventral root of the transverse process. Xenarthrous articulations cannot be seen because of fragmentation. Metapophyses are preserved on the two posterior vertebrae between the neural spine and the transverse process, projecting anteriorly over the preceding vertebra. In *D. novemcinctus*, *D. septemcinctus*, and *D. hybridus*, the seventh thoracic vertebra is the anterior-most bearing metapophyses, whereas in *P. grandis* metapophyses first appear on the eighth.

The three partial ribs have slim bodies with several rounded concavities for muscular attachment. Their anterior surfaces bear an elongated sulcus. A shallow neck separates the articular facets of the capitulum and tuberculum.

Lumbar and Sacral Vertebrae—Four posterior-most lumbar vertebrae, two anterior-most sacral vertebrae, and the complete right ilium are associated (Fig. 6G, H). In relation to the thoracic elements, the lumbar vertebrae have taller centra and more ventral transverse processes. The distal extremities of the neural spines, metapophyses, and transverse processes are missing. Epiphyses are not entirely fused to their respective centra and sediment occupies the space that once housed the intervertebral discs. Neural spines are markedly angled posteriorly, whereas the metapophyses project anteriorly. Xenarthrous articulations are conspicuous, including those between the last lumbar and the first sacral vertebrae. The general morphology of the articulations is consistent with that described by Gaudin (1999). The two preserved sacral vertebrae (S1 and S2) lack most of their left side. Besides the anterior epiphysis of the centrum of S1, there is another unfused epiphysis between the posterior part of the transverse process and the ilium. S1 is broader than S2, and the aliform transverse process represents most of the contact with the ilium. The metapophyses of S1 in *D. punctatus* are more developed than those of *D. novemcinctus*, as also recognized by Winge (1915). The dorsal spinal nerve foramen is on the suture between the transverse processes of S1 and S2, more laterally positioned than in *D. novemcinctus*. The sacral elements project dorsally at an obtuse angle to the lumbar series. In *P. grandis*, the anterior border of the sacroischiadic foramen is in line with S3/S4 suture, more posterior than in *D. novemcinctus*, *D. hybridus*, and *D. septemcinctus*, where it lies at the level of S2.

Scapula and Forelimb—Only the ventral portion of left scapula is represented (Fig. 7A, B). The glenoid cavity is elongated, slightly concave, and separated from the coracoid process by a delicate sulcus. On the external surface, the spine has a concave ventral border and is distally fragmented. Two grooves for muscular attachment are on the posterior border of the bone.

The almost complete left humerus (Fig. 7C, D) bears unfused proximal and distal epiphyses. It is as robust as that of *P. grandis*, but distally wider than in other Dasypodini. A shallow neck separates the diaphysis from the head, which appears to be equivalent in size to the greater tuberosity. The lesser tuberosity is gracile. The bicipital groove separates both tuberosities; it extends over the shaft and has numerous foramina. The deltopectoral crest occupies almost half of the shaft, which flattens toward the distal end. The entepicondylar foramen is elongated in the plane of the entepicondylar bridge, and the coronoid fossa is mediolaterally expanded. The supinator crest ends above the thin ectepicondyle, which is already co-ossified to the diaphysis, in contrast to the entepicondyle. A delicate groove in the trochlea separates ulnar and radial facets. In posterior view, the olecranon fossa is observed.

The almost complete ulna (Fig. 7E, F) also has unfused proximal and distal epiphyses. As in other *Dasypus*, the olecranon corresponds to half of the ulnar length, and broad sulci extend along its medial and lateral borders. A transverse crest separates the articular facet for the radius from the sigmoid cavity. The coronoid process projects medially, and a deep groove lies distally. The interosseous crest extends over the whole anterior border of the shaft and ends distally in a flattened facet for the radius. The distal epiphysis bears a convex articular facet, with no styloid process. In contrast, *D. novemcinctus* shows a lateral crest on the distal shaft and more delicate ridges surround the articular facet for the radius.

Originally, the left manus (Fig. 7G) was reconstituted with some mistakes in a block of plaster, maintained because of the historical value of the specimen. Four elements are proximal to the metacarpals: two proximal phalanges incorrectly identified as carpals, the semilunar (or lunate), and the pisiform. Compared with the relatively smaller and more gracile pisiform of *D. hybridus* and *D. novemcinctus*, the robust triangular morphology of latter bone in MN 552-V resembles that of *Stegotherium tauberi* (Scott, 1903–1904). We could not compare it with the pisiform of other extant *Dasypus*, and it is not preserved in *P. grandis*. First, second, and third metacarpals are preserved. The first has two proximal concave facets and articulates laterally with the second metacarpal, which is twice as long. The second and the much longer third metacarpal show unfused distal epiphyses and are concave along their medial and lateral borders. Second and

← FIGURE 6. Postcranial elements of *Dasypus punctatus*, MN 552-V. Cervical vertebrae in dorsal (**A**) and ventral (**B**) views; isolated fifth (?) thoracic vertebra in anterior (**C**) and posterior (**D**) views; association of thoracic vertebrae and ribs in dorsal (**E**) and right lateral (**F**) views; lumbar vertebrae, sacral vertebrae, and ilium in right lateral (**G**) and dorsal (**H**) views. **Abbreviations**: **an**, anapophysis; **At**, atlas; **Axi**, axis; **ax/px1** and **ax/px2**, dorsal and ventral xenartrous intervertebral joints, respectively; **C3**, **C4**, and **C5**, third, fourth, and fifth cervical vertebrae, respectively; **dn**, dorsal spinal nerve foramen; **fa**, facet for the atlas; **fax**, facet for the axis; **fc**, facet for the occipital condyle; **fcr**, facet for the capitulum of rib; **ftr**, facet for the tuberculum of rib; **fv**, facet for preceding vertebra; **il**, ilium; **mt**, metapophysis; **ns**, neural spine; **op**, odontoid process; **os**, osteoderm; **pr**, prezygapophysis; **pz**, postzygapophysis; **rb**, rib; **S1** and **S2**, first and second sacral vertebrae, respectively; **sn**, foramen for emergence of spinal nerve; **vc**, vertebroarterial canal. Scale bars equal 10 mm.

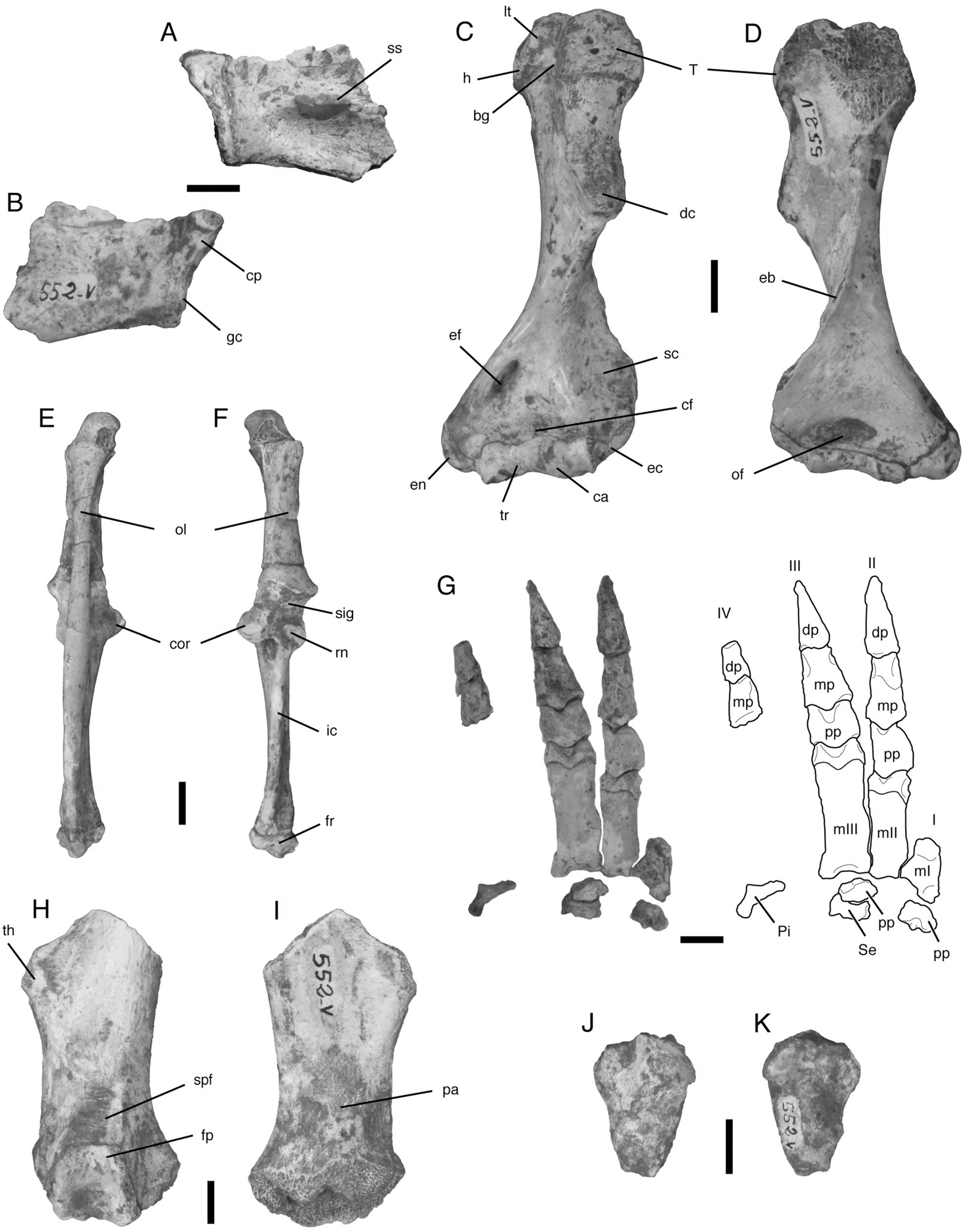

FIGURE 7. Postcranial elements of *Dasypus punctatus*, MN 552-V. Scapula in external (**A**) and internal (**B**) views; humerus in anterior (**C**) and posterior (**D**) views; ulna in posterior (**E**) and anterior (**F**) views; manus in dorsal view (**G**); femur in anterior (**H**) and posterior (**I**) views; patella in anterior (**J**) and posterior (**K**) views. **Abbreviations**: **bg**, bicipital groove; **ca**, capitulum; **cf**, coronoid fossa; **cor**, coronoid process; **cp**, coracoid process; **dc**, deltopectoral crest; **dp**, distal phalanx; **eb**, entepicondylar bridge; **ec**, ectepicondyle; **ef**, entepcondylar foramen; **en**, entepicondyle; **fp**, facet for the patella; **fr**, facet for the radius; **gc**, glenoid cavity; **h**, head; **ic**, interosseous crest; **lt**, lesser tuberosity; **m**, metacarpal; **mp**, middle phalanx; **of**, olecranon fossa; **ol**, olecranon; **pa**, popliteal area; **Pi**; pisiform; **pp**, proximal phalanx; **rn**, radial notch; **sc**, supinator crest; **Se**, semilunar (= lunate); **sig**, sigmoid cavity; **spf**, suprapatellar fossa; **ss**, spine of scapula; **T**, greater tuberosity; **th**, third trochanter; **tr**, trochlea. Scale bars equal 10 mm.

TABLE 5. Measurements (mm) of the most complete postcranial remains of *D. punctatus*.

Element	GL	GW	DV	LC	WC	DC	PW	DW
Atlas	17.0	39.7	22.3					
C2		31.0		21.0*				
C3				12.2				
C4				9.7		2.9		
C5				8.6		3.7		
Thoracic vertebrae				9.6–14.0	12.0–16.6	6.6–7.6		
Lumbar vertebrae				16.1–17.2	16.6–19.0	7.9**		
S1				18.0				
Ilium	87.2							38.6
Humerus	87.5						27.5	37.6
Ulna	102.5						7.9	9.8
Metacarpal I	14.5						9.5	5.5
Metacarpal II	25.3						6.9	8.9
Metacarpal III	33.1						11.4	9.6
Patella	22.6						17.8	7.1

*Including odontoid process; **measured on the anterior-most lumbar vertebra preserved. **Abbreviations**: **DC**, maximum depth of vertebral centrum; **DV**, dorsoventral diameter; **DW**, maximum distal width; **GL**, greatest length; **GW**, greatest width, including transverse processes; **LC**, length of vertebral centrum; **PW**, maximum proximal width; **WC**, width of vertebral centrum.

third digits are complete, whereas the fourth did not preserve the proximal phalanx. The proximal phalanges are the shortest digital elements, and the distal phalanges (ungual) taper distally. In the fourth digit, the middle phalanx is smaller and more laterally compressed than in the other digits. As in *D. novemcinctus*, the third ray is the most robust, followed by the second. Except for *D. kappleri*, the fifth digit is considered absent or reduced to rudimentary bony elements in *Dasypus* (Flower, 1885; Schulthess, 1920), but a recent study (Costa and Vizcaíno, 2010) questions their assertion.

Ilium and Hind Limb—The right ilium is associated with the lumbar and sacral vertebrae (Fig. 6G, H). The body is cylindrical along the medial border, becoming gradually dorsoventrally compressed laterally, and ending in a sharp iliac crest. It widens posteriorly toward the unfused epiphysis, which is roughly triangular. Dorsally, the anterior half of the ilium is markedly concave. Although lacking the posterior sacral vertebrae, the articulation for the sacrum clearly narrows towards the rear. The ilium of *P. grandis* is more robust than that of *D. punctatus* and modern *Dasypus*.

The right femur is poorly represented, preserving only the distal half of the bone without part of the epiphysis (Fig. 7H, I). The distal part of the shaft is compressed anteroposteriorly and broken just proximal to the level of the third trochanter. It bears the suprapatellar fossa on the anterior surface and a rugose popliteal area on the posterior. Prominent crests delimit the facet for the patella in the partial distal epiphysis.

The complete right patella (Fig. 7J, K) is subtriangular. On its proximal surface, two fossae flank an anteriorly rounded apophysis. Except for a flat striated area on the apex, the anterior surface is convex. A longitudinal ridge delimits the two posterior facets—an almost flat medial facet and a larger lateral facet, which has a very excavated surface, as in extant *Dasypus*.

Table 5 includes relevant measurements of the most complete postcranial elements of MN 552-V.

PHYLOGENETIC ANALYSIS

The present study of MN 552-V is related to three main taxonomic questions, already presented by previous authors: (1) the possible allocation of *Dasypus punctatus* to the genus *Propraopus* (proposed by Hoffstetter, 1952, and generally followed since); (2) the putative close relationship of *D. kappleri* to the extinct *D. bellus* and *Propraopus*, including *P. punctatus* (pointed by Rincón et al., 2008); and (3) the possible synonymy between *Propraopus sulcatus* and *Propraopus grandis* (suggested by Hoffstetter, 1952, and Paula-Couto, 1982). In order to answer these questions, we tested the possible affinities of MN 552-V within Dasypodini in the cladistic analysis presented below.

Eighteen morphological characters were scored for seven ingroup taxa (Appendices 1–3), namely: *Dasypus punctatus*, based on MN 552-V; the extant *Dasypus hybridus*, *D. kappleri*, *D. novemcinctus*, and *D. septemcinctus*, based on several specimens; *Propraopus grandis*, based on MLP 69-IX-9-9 (an almost complete carapace) and MACN 17989 (skull, postcranial elements, and carapace fragments), which were grouped based on the matching morphology of their osteoderms; and *Propraopus sulcatus*, based on numerous osteoderms figured by Winge (1915:pl. V.3, 4), which agree in morphology, although they come from different sites in the Lagoa Santa karst. The osteoderms of *Dasypus punctatus* studied by Lund (1840) and figured by Winge (1915) were not included in the analysis, because they agree with those of MN 552-V, which is a more complete specimen.

The outgroup was composed of two taxa, *Stegotherium tauberi* and *Anadasypus hondanus* Carlini, Vizcaíno, and Scillato-Yané, 1997. The former was scored based on replicas and photos of the material studied by Scott (1903–1904), named *Stegotherium tesselatum* therein (but see González and Scillato-Yané, 2008 for the taxonomic update). Previous phylogenetic studies (Engelmann, 1985; Abrantes and Bergqvist, 2006; Gaudin and Wible, 2006) found *Stegotherium* and *Dasypus* to be sister taxa. However, *Stegotherium* has an extremely distinct carapace, precluding adequate comparisons with the ingroup: it does not have an scapular buckler and the presence of a pelvic buckler is uncertain; also, there is no principal sulcus in the movable osteoderms (Scott, 1903–1904; González and Scillato-Yané, 2008). Therefore, the holotype (IGM 183499) of *Anadasypus hondanus*, the oldest known Dasypodini, was added to the outgroup. The synapomorphies of the ingroup are principal sulcus/sulci of movable osteoderms reaching the posterior border; subcircular principal sulcus of buckler osteoderms; and peripheral figures present in the anterior row of each caudal ring (Carlini et al., 1997).

Except for *S. tauberi* and *P. sulcatus*, the characters were scored based on direct observation of specimens (see Appendix 1). Ten characters are related to the cranial anatomy and eight to the osteoderms. Five characters were defined as multistate. Following the maximum parsimony criterion, an exact analysis was conducted using TNT 1.1 (Goloboff et al., 2008).

With multistate characters treated as non-additive, a single most parsimonious tree (MPT) was found (tree length = 28; CI = 0.86; RI = 0.83; Fig. 8). It includes two main clades: one

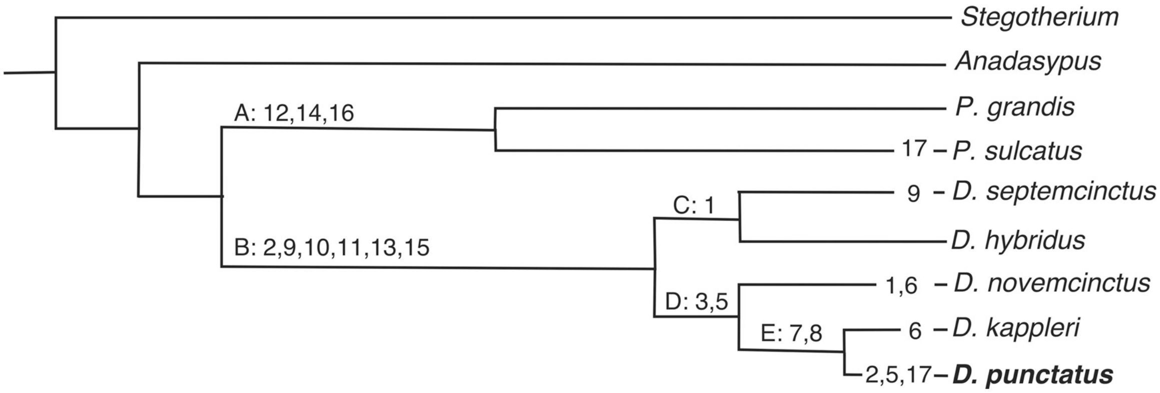

FIGURE 8. Most parsimonious tree resulting from the cladistic analysis of 18 characters scored for nine dasypodine taxa. *Stegotherium* and *Anadasypus* compose the outgroup. Capital letters represent the nodes discussed in the text, followed by a list of their apomorphic characters identified by the numbers assigned them in Appendix 2. Tree length = 28; CI = 0.86; RI = 0.83.

comprising *P. grandis* and *P. sulcatus* (node A, supported by characters 12[1], 14[0], and 16[0]) and another grouping MN 552-V and the living species of *Dasypus* (node B, supported by characters 2[1], 9[1–2], 10[1], 11[1], 13[1], and 15[1]). In addition, the analysis yielded a sister-taxon relationship between MN 552-V and *D. kappleri* (node E, supported by characters 7[1] and 8[1]). Furthermore, MN 552-V, *D. kappleri*, and *D. novemcinctus* (node D, characters 3[1] and 5[2]), as well as *Dasypus septemcinctus* and *D. hybridus* (node C, character 1[0]), formed weakly supported clades. A second analysis performed with the multistate characters treated as additive yielded the same MPT (tree length = 29).

DISCUSSION

The strongly supported two-fold division of the ingroup taxa has taxonomic and nomenclatural implications. Because node A encompasses the type species of *Propraopus* (i.e., *P. grandis*), this generic assignation should be applied to it, whereas node B corresponds to *Dasypus*, because it encompasses its type species (i.e., *D. novemcinctus*), the other living species of Dasypodini analyzed, as well as MN 552-V. The latter specimen matches the anatomy of the material ascribed by Lund (1840) to *D. punctatus*, including the lectotype designated herein, and the nomenclature originally adopted by that author better fits the hypothesis of relationships proposed here. In contrast, *P. sulcatus* is better attributed to *Propraopus*, as proposed by Hoffstetter (1952).

Our phylogeny contradicts the idea of Rincón et al. (2008) that *Dasypus kappleri* and *Propraopus* are grouped within Dasypodini, given that *Propraopus* forms a discrete clade, separate from *D. kappleri* in our the tree. On the other hand, affinities between *D. kappleri* and *D. punctatus* are supported by a strongly keeled posterodorsal border of the palate and completely flat palatines (characters 7[1] and 8[1], respectively; node E). Comparing with the systematics of extant *Dasypus*, the subgenus that contains only *D. kappleri* is defined by keeled posterodorsal border of the palate, condylonasal length greater than 111 mm, and presence of the fifth digit in the manus (Wetzel, 1985). With an estimated skull length of 119 mm (Table 4), *Dasypus punctatus* also matches the second feature. The significance of the reduction of fifth digit in most living *Dasypus* is controversial (Wetzel and Mondolfi, 1979; Costa and Vizcaíno, 2010); unfortunately, the incomplete manus of MN 552-V does not elucidate this question. Because *D. bellus* was not included in our phylogeny, we cannot address its potential affinities to either *Propraopus* or the *D. kappleri*/*D. punctatus* clade.

As for the possible synonymy between *P. grandis* and *P. sulcatus*, these differ on a single character in the analysis (total number of foramina in the principal sulci of movable osteoderms, character 17). Oliveira and Pereira (2009) listed potential autapomorphies of *P. sulcatus*, but some are also seen in *P. grandis* (e.g., subcircular to hexagonal principal figure in buckler osteoderms; movable osteoderms with principal sulci forming a lageniform figure). Comprehensive first-hand analyses of *P. sulcatus* and *P. magnus* are needed to fully address this question, but this is beyond the scope of the present study.

In our study, the osteoderms were essential to define the relationships among taxa, counterbalancing the extremely conservative anatomy of the skull and postcranium. These are the elements most frequently preserved as fossil for cingulates and historically underlie the systematics of the group (e.g., Ameghino, 1902; Simpson 1948; Scillato-Yané, 1982; Vizcaíno, 1994; Carlini et al., 1997, 2010). However, the inclusion of osteoderm characters in phylogenetic studies is still scarce (Abrantes and Bergqvist, 2006; Croft et al., 2007; Ciancio, 2010). Despite recent criticisms against scoring characters based on isolated osteoderms (Porpino et al., 2009), the analysis of carapace fragments, together with a careful evaluation of the morphologic variation among different portions of the carapace, allows reliable comparisons.

CONCLUSIONS

Dasypus punctatus is considered the valid name for the species sometimes identified as *Propraopus punctatus*, and its lectotype was designated here based on the syntypes figured by Winge (1915). MN 552-V is assigned to *D. punctatus* based on the anatomical traits it shares exclusively with the type material of that taxon, i.e., particularly numerous foramina in both buckler and movable osteoderms. A cladistic analysis indicates the existence of two well-supported clades: one composed by *D. punctatus* and living species of *Dasypus*, and another by the extinct *Propraopus grandis* and *P. sulcatus*. Therefore, the genus *Propraopus* as defined by Hoffstetter (1952) circumscribes a polyphyletic array of taxa, and the original attribution (Lund, 1840) is preferred for *D. punctatus*. Previously suggested affinities between *D. kappleri* and *D. punctatus* (but not *Propraopus*) are corroborated.

ACKNOWLEDGMENTS

We are grateful to K. L. Hansen (ZMK) for helpful information and photos of the lectotype; to S. A. K. de Azevedo and D. Henriques (MNRJ), M. de Vivo (MZUSP), A. Kramarz (MACN), and A. I. Olivares, D. Verzi, and M. Reguero (MLP) for allowing the study of material under their care; to S. Hirooka and E. M. Silva (CC) for photos of the Rosário do Oeste specimens; to L. R. González (MLP) for sharing photos of *Stegotherium*, and to C. A. Norris (YPM-PU) for authorizing it; and to the Willi Hennig Society for making TNT software freely available. We also thank A. A. Carlini, the reviewers (É. V. Oliveira and T. J. Gaudin), and the editor (T. Martin) for constructive suggestions on the manuscript. FAPESP (Proc. 07/52970-2) and CAPES (Proc. BEX 0840/10-6) grants to M. C. Castro supported this research.

LITERATURE CITED

Abrantes, É. A. L., and L. P. Bergqvist. 2004. Proposta filogenética para os Dasypodidae (Mammalia: Cingulata); pp. 261–274 in V. Gallo, P. M. Brito, H. M. A. Silva, and F. J. Figueiredo (eds.), Paleontologia de Vertebrados: Grandes Temas e Contribuições Científicas. Interciências, Rio de Janeiro.

Aguiar, J. M., and G. A. B da Fonseca. 2008. Conservation status of the Xenarthra; pp. 215–231. in S. F. Vizcaíno and W. J. Loughry (eds.), The Biology of the Xenarthra. University Press of Florida, Gainesville, Florida.

Ameghino, F. 1881. La Antiguedad del Hombre en el Plata, Volume 2. Masson-Igon Hermanos, Paris and Buenos Aires, 557 pp.

Ameghino, F. 1902. Notices préliminaires sur des mammiféres nouveaux des terrains crétacés de Patagonie. Boletín de la Academia Nacional de Ciencias de Córdoba 17:5–73.

Auler, A. S., L. B. Piló, P. L. Smart, X. F. Wang, D. Hoffmann, D. A. Richards, R. L. Edwards, W. A. Neves, and H. Cheng. 2006. U-series dating and taphonomy of Quaternary vertebrates from Brazilian caves. Palaeogeography, Palaeoclimatology, Palaeoecology 240:508–522.

Bergqvist, L. P., É. A. L. Abrantes, and L. D. Avilla. 2004. The Xenarthra (Mammalia) of São José de Itaboraí Basin (upper Paleocene, Itaboraian), Rio de Janeiro, Brazil. Geodiversitas 26:323–337.

Carlini, A. A., and G. J. Scillato-Yané. 1999. Cingulata del Oligoceno de Salla, Bolivia. Congreso Internacional Evolución Neotropical del Cenozoico, La Paz, Bolivia, 19–22 May 1999. Programas y Resúmenes:15A.

Carlini, A. A., M. R. Ciancio, and G. J. Scillato-Yané. 2010. Middle Eocene–Early Miocene Dasypodidae (Xenarthra) of southern South America: faunal succession at Gran Barranca—biostratigraphy and paleoecology; pp. 106–129 in R. H. Madden, A. A. Carlini, M. G. Vucetich, and R. F. Kay (eds.), The Paleontology of Gran Barranca: Evolution and Environmental Change through the Middle Cenozoic of Patagonia. Cambridge University Press, Cambridge, U.K.

Carlini, A. A., S. F. Vizcaíno, and G. J. Scillato-Yané. 1997. Armored xenarthrans: a unique taxonomic and ecologic assemblage; pp. 213–226 in R. F. Kay, R. H. Madden, R. Cifelli, and J. J. Flynn (eds.), Vertebrate Paleontology in the Neotropics. The Miocene Fauna of La Venta, Colombia. Smithsonian Institution Press, Washington, D.C. and London.

Cartelle, C. 1999. Pleistocene mammals of the Cerrado and Caatinga of Brazil; pp. 27–46 in J. F. Eisenberg and K. H. Redford (eds.), Mammals of the Neotropics. The University of Chicago Press, Chicago, Illinois.

Cartelle, C., and S. Hirooka. 2005. The first record of *Pteronura brasiliensis* (Gmelin, 1788) (Carnivora, Mustelidae) from the Pleistocene. Arquivos do Museu Nacional Rio de Janeiro 63:595–598.

Castellanos, A. 1925. Un nuevo dasipodino extinguido en la parte meridional de Bolívia, *Dasypodon atavus* n. g. et n. sp. Annales del Museo Nacional de Historia Natural de Buenos Aires "Bernardino Rivadavia" 33:255–285.

Castro, M. C., and J. Ferigolo. 2010. More strange joints in Dasypodidae: additional articulations in cervical and thoracic vertebrae. Abstracts of the Ninth International Congress of Vertebrate Morphology, Punta del Este, Uruguay, 26–31 July 2010. Abstract 152.

Ciancio, M. R. 2010. Los Dasypodoidea (Mammalia, Xenarthra) del Deseadense (Oligoceno) de América del Sur—su importancia filogenética y bioestratigráfica. Ph.D. dissertation, Universidad Nacional de La Plata, La Plata, Buenos Aires, 290 pp.

Ciancio, M. R., M. C. Castro, F. C. Galliari, A. A. Carlini, and R. J. Asher. 2012. Evolutionary implications of dental eruption in *Dasypus* (Xenarthra). Journal of Mammalian Evolution 19:1–8.

Cione, A. L., and E. P. Tonni. 2005. Bioestratigrafia basada en Mamíferos del Cenozóico Superior de la Província de Buenos Aires, Argentina; pp. 183–200 in R. E. De Barrio, R. O. Etcheverry, M. F. Caballé, and E. Llambias (eds.), Geología y Recursos Minerales de la Provincia de Buenos Aires: Relatorio del XVI Congreso Geológico Argentino, La Plata, 20–23 September 2005.

Cope, E. D. 1889. The Edentata of North America. American Naturalist 23:657–664.

Costa, F. R., and S. F. Vizcaíno. 2010. A diagnostic character revisited: is there a fifth toe in the forefoot of *Dasypus novemcinctus* (Xenarthra: Dasypodidae)? Zootaxa 2671:61–64.

Croft, D. A., J. J. Flynn, and A. R. Wyss. 2007. A new basal glyptodontid and other Xenarthra of the early Miocene Chucal fauna, Northern Chile. Journal of Vertebrate Paleontology 27:781–797.

Delsuc, F., M. Superina, M. K. Tilak, E. J. P. Douzery, and A. Hassanin. 2012. Molecular phylogenetics unveils the ancient evolutionary origins of the enigmatic fairy armadillos. Molecular Phylogenetics and Evolution 62:673–680.

Downing, K. F., and R. S. White. 1995. The cingulates (Xenarthra) of the Leisey Shell Pit local fauna (Irvingtonian), Hillsborough County, Florida. Bulletin of the Florida Museum of Natural History 37:375–396.

Engelmann, G. F. 1985. The phylogeny of the Xenarthra; pp. 51–63 in G. G. Montgomery (ed.), The Evolution and Ecology of Armadillos, Sloths, and Vermilinguas. Smithsonian Institution, Washington, D.C.

Faure, M., C. Guérin, and F. Parenti. 1999. The Holocene megafauna from Toca do Serrote do Artur (São Raimundo Notato archaeological area, Piauí, Brazil). Comptes Rendus de l'Academie des Sciences, Series IIA—Earth and Planetary Science 329:443–448.

Ferigolo, J. 1981. Osteologia do sincranio e odontologia de *Euphractus sexcinctus* Linnaeus, 1758 (Xenarthra, Mammalia). M.S. thesis, Universidade Federal do Rio Grande do Sul, Porto Alegre, Rio Grande do Sul, 311 pp.

Flower, W. H. 1885. An Introduction to the Osteology of the Mammalia. Macmillan & Co., London, 344 pp.

Galliari, F. C., A. A. Carlini, and M. R. Sánchez-Villagra. 2010. Evolution of the axial skeleton in armadillos (Mammalia, Dasypodidae). Mammalian Biology 75:326–333.

Gaudin, T. J. 1999. The morphology of xenarthrous vertebrae (Mammalia, Xenarthra). Fieldiana: Geology 41:1–38.

Gaudin, T. J., and J. R. Wible. 2006. The phylogeny of living and extinct armadillos (Mammalia, Xenarthra, Cingulata): a craniodental analysis; pp. 153–198 in M. T. Carrano, T. J. Gaudin, R. W. Blob, and J. R. Wible (eds.), Amniote Paleobiology: Perspectives on the Evolution of Mammals, Birds and Reptiles. University of Chicago Press, Chicago, Illinois.

Goloboff, P., J. Farris, and K. Nixon. 2008. TNT: a free program for phylogenetic analysis. Cladistics 24:774–786.

González, L. R., and G. J. Scillato-Yané. 2008. A new species of *Stegotherium* Ameghino (Xenarthra, Dasypodidae, Stegotheriini) from the Miocene of Santa Cruz Province (Argentina). Ameghiniana 45:641–648.

Gray, J. E. 1821. On the natural arrangement of vertebrose animals. London Medical Repository 15:296–310.

Guth, C. 1961. La Region Temporale des Édentés. Imprimerie Jeanne D'arc Le Puy, Paris, 207 pp.

Hill, R. V. 2006. Comparative anatomy and histology of xenarthran osteoderms. Journal of Morphology 267:1441–1460.

Hoffstetter, R. 1952. Les Mammifères pléistocènes de la Republique de l'Equateur. Memoires de la Société Géologique de France, Nouvelle Serie 31:1–391.

Hoffstetter, R. 1958. Xenarthra; pp. 535–636 in J. Piveteau (ed.), Traité de Paléontologie. Masson et Cie, Paris.

Hubbe, A., M. Hubbe, and W. Neves. 2007. Early holocene survival of megafauna in South America. Journal of Biogeography 34:1642–1646.

Hubbe, A., M. Hubbe, and W. Neves. 2009. New Late-Pleistocene dates for the extinct megafauna of Lagoa Santa, Brazil. Current Research in the Pleistocene 26:154–156.

Illiger, C. 1811. Prodromus Systematis Mammalium et Avium Additis Terminis Zoographicis Utriusque Classis. C. Salfeld, Berlin, 301 pp.

Krmpotic, C. M., M. R. Ciancio, C. Barbeito, R. C. Mario, and A. A. Carlini. 2009. Osteoderm morphology in recent and fossil euphractine xenarthrans. Acta Zoologica 90:339–351.

Linnaeus, C. 1758. Systema Naturae (per Regna Tria Naturae, Secundum Classis, Ordines, Genera, Species cum Characteribus, Differentiis, Synonymis, Locis). Tenth edition, Volume 1. Laurentii Salvii, Stockholm, 824 pp.

Lund, P. W. 1840. Blik paa Brasiliens Dyreverden för Sidste Jordomvaeltning. Treide Afhandling: Forsaettelse af Pattedyrene. Det Kongelige Danske Videnskabernes Selskbas Naturvidenskabelige og Mathematiske Afhandlinger 8:217–272.

Lund, P. W. 1842. Blik paa Brasiliens Dyreverden för Sidste Jordomvaeltning. Fjerde Afhandling: Forstsaettelse af Pattedyrene. Det Kongelige Danske Videnskabernes Selskabs Naturnvidenskabelige og Mathematiske Afhandlinger 9:137–208.

Macrini, T. 2005. *Dasypus novemcinctus*. Digital Morphology. Available at http://digimorph.org/specimens/Dasypus_novemcinctus/. Accessed May 5, 2012.

Marshall, L. G., and T. Sempere. 1991. The Eocene to Pleistocene vertebrates of Bolivia and their stratigraphic context: a review; pp. 631–652 in R. Suárez-Soruco (ed.), Fosiles y Facies de Bolivia: Vertebrados. Yacimentos Petrolíferos Fiscales Bolivianos, Santa Cruz.

Marshall, L. G., A. Berta, R. Hoffstetter, R. Pascual, O. A. Reig, M. Bombin, and A. Mones. 1984. Mammals and stratigraphy: geochronology of the continental mammal-bearing Quaternary of South America. Palaeovertebrata, Mémoire Extraordinaire:1–76.

Martin, B. E. 1916. Tooth development in *Dasypus novemcinctus*. Journal of Morphology 27:647–691.

McKenna, M. C., and S. K. Bell. 1997. Classification of Mammals above the Species Level. Columbia University Press, New York, 640 pp.

Neves, W. A., and L. B. Piló. 2003. Solving Lund's dilemma: new AMS dates confirm that humans and megafauna coexisted at Lagoa Santa. Current Research in the Pleistocene 20:57–60.

Oliveira, É. V., and L. P. Bergqvist. 1998. A new Paleocene armadillo (Mammalia, Dasypodoidea) from the Itaboraí Basin, Brazil. Paleogene in South America and the Antarctic Pennisula. Asociación Paleontológica Argentina, Publicación E special 5:35–40.

Oliveira, É. V., and J. C. Pereira. 2009. Intertropical cingulates (Mammalia, Xenarthra) from the Quaternary of Southern Brazil: systematic and paleobiogeographical aspects. Revista Brasileira de Paleontologia 12:167–178.

Oliveira, É. V., A. M. Ribeiro, and L. P. Bergqvist. 1997. A new Oligocene cingulate (Mammalia: Xenarthra) from the Taubaté Basin, Brazil. Anais da Academia Brasileira de Ciências 69:461–470.

Paula-Couto, C. 1973. Edentados fósseis de São Paulo. Anais da Academia Brasileira de Ciências 45:261–275.

Paula-Couto, C. 1979. Tratado de Paleomastozoologia. Academia Brasileira de Ciências, Rio de Janeiro, 590 pp.

Paula-Couto, C. 1980. *Propraopus punctatus* (Lund, 1840) no Pleistoceno de Cerca Grande, Minas Gerais. Anais da Academia Brasileira de Ciências 52:323–325.

Paula-Couto, C. 1982. Pleistocene armadillo from Cantagalo, State of Rio de Janeiro. Iheringia, Série Geologia 7:65–68.

Paula-Couto, C. 1983. Fossil mammals from the Cenozoic of Acre, Brazil, VI – Edentata Cingulata. Iheringia, Série Geologia 8:33–49.

Pessôa, J. B., D. T. Lima, É. A. L. Abrantes, K. O. Porpino, and L. S. Avilla. 2008. Systematic revision of long-nosed armadillos (Mammalia, Cingulata, Dasypodidae). Boletim de Resumos do VI Simpósio Brasileiro de Paleontologia de Vertebrados. Paleontologia em Destaque Edição Especial:161–162.

Porpino, K. D., J. C. Fernicola, and L. P. Bergqvist. 2009. A new cingulate (Mammalia: Xenarthra), *Pachyarmatherium brasiliense* sp nov., from the late Pleistocene of Northeastern Brazil. Journal of Vertebrate Paleontology 29:881–893.

Rincón, A. D., R. S. White, and H. G. McDonald. 2008. Late Pleistocene cingulates (Mammalia: Xenarthra) from Mene de Inciarte tar pits, Sierra de Perijá, western Venezuela. Journal of Vertebrate Paleontology 28:197–207.

Schulthess, B. 1920. Beiträge zur Kenntnis der Xenarthra auf Grund der "Santiago Roth'schen Sammlung" des Zoologischen Museum der Universität Zürich. Abhandlungen der Schweizerischen Palaeontologischen Gesellschaft 44:1–119.

Scillato-Yané, G. J. 1976. Dasypodidae from Riochican of Itaboraí (Brazil). Anais da Academia Brasileira de Ciências 48:527–530.

Scillato-Yané, G. J. 1982. Los Dasypodidae (Mammalia, Edentata) del Plioceno y Pleistoceno de Argentina. Ph.D. dissertation, Universidad Nacional de La Plata, La Plata, Buenos Aires, 159 pp.

Scott, W. B. 1903–1904. Mammalia of the Santa Cruz Beds. Part 1: Edentata. Reports of the Princeton University Expeditions to Patagonia 5:1–364.

Simpson, G. G. 1929. Pleistocene mammalian fauna of the Seminole Field, Pinellas County, Florida. Bulletin of the American Museum of Natural History 56:561–599.

Simpson, G. G. 1948. The beginning of the Age of Mammals in South America. Part I. Introduction, Edentata, Condylarthra, Litopterna, and Notioprogonia. Bulletin of the American Museum of Natural History 91:1–232.

Tejedor, M. F., F. J. Goin, J. N. Gelfo, G. Lopez, M. Bond, A. A. Carlini, G. J. Scillato-Yané, M. O. Woodburne, L. Chornogubsky, E. Aragon, M. A. Reguero, N. J. Czaplewski, S. Vincon, G. M. Martin, and M. R. Ciancio. 2009. New Early Eocene mammalian fauna from western Patagonia, Argentina. American Museum Novitates 3638:1–43.

Ubilla, M., and D. Perea. 1999. Quaternary vertebrates of Uruguay: a biostratigraphic, biogeographic and climatic overview; pp. 75–90 in J. Rabassa and M. Salemme (eds.), Quaternary of South America and Antarctic Peninsula. A. A. Balkema, Rotterdam.

Vickaryous, M. K., and B. K. Hall. 2006. Osteoderm morphology and development in the nine-banded armadillo, *Dasypus novemcinctus* (Mammalia, Xenarthra, Cingulata). Journal of Morphology 267:1273–1283.

Vizcaíno, S. F. 1994. Systematics and anatomy of the Astegotheriini Ameghino 1906 (new rank) (Xenarthra, Dasypodidae, Dasypodinae). Ameghiniana 31:3–13.

Wetzel, R. M. 1985. Taxonomy and distribution of armadillos; pp. 23–46 in G. G. Montgomery (ed.), The Evolution and Ecology of Armadillos, Sloths, and Vermilinguas. Smithsonian Institution Press, Washington, D.C.

Wetzel, R. M., and E. Mondolfi. 1979. The subgenera and species of long-nosed armadillos, genus *Dasypus*; pp. 43–63 in J. F. Eisenberg (ed.), Vertebrate Ecology in the Northern Neotropics. Smithsonian Institution Press, Washington, D.C.

Wible, J. R., and T. J. Gaudin. 2004. On the cranial osteology of the yellow armadillo *Euphractus sexcinctus* (Dasypodidae, Xenarthra, Placentalia). Annals of Carnegie Museum 73:260–260.

Wilson, D. E., and D. M. Reeder. 2005. Mammals Species of the World: A Taxonomic and Geographic Reference, third edition. Johns Hopkins University Press, Baltimore, Maryland, 2122 pp.

Winge, H. 1915. Jordfunde og nulevende Gumlere (Edentata) fra Lagoa Santa, Minas Geraes, Brasilien. E. Museo Lundii 3:1–321.

Wolf, T. 1875. Geognostische Mittheilungen aus Ecuador. 4: Kritische Zusammenstellung der in Ecuador stattgefundenen Vulkan-Ausbrüche und Erdbeben seit der Zeit der Conquista. Neues Jahrbuch für Mineralogie, Geologie und Paläontologie 1875:152–170.

Submitted March 5, 2012; revisions received July 29, 2012; accepted September 8, 2012.

Handling editor: Thomas Martin.

APPENDIX 1. Specimens examined for comparative study and cladistic analysis.

Anadasypus hondanus: IGM 183499 (holotype).

Dasypus hybridus: MLP 1-I-03-65, 3-X-96-1.

Dasypus kappleri: MZUSP 8950, 24798.

Dasypus novemcinctus: MCN-MA 99, 986, 2788, 2836, 3021, MZUSP 7996, 10431, 13800, 13801, 20189.

Dasypus septemcinctus: MZUSP 5111, 8111, 19983, 19984.

Dasypus punctatus: MN 552-V, MCN-PV 009, 014.

Dasypus yepesi: MLP 30-III-90-2, 30-III-90-3, 30-III-90-4, 30-III-90-5, 30-III-90-8 (holotype).

Propraopus grandis: MACN 1610, 1630, 7027, 17989, MACN-A 1170, 10989, 11108, MLP 58-IX-3-26, 69-IX-9-9, 90-V-1-4.

Propraopus sulcatus: photos in Winge (1915:pl. V.3, 4).

Stegotherium tauberi: YPM-PU 15565, 15566 (replicas and photos).

APPENDIX 2. List of character and character states used in the cladistic analysis. Characters marked with an asterisk (*) are multistate.

(1)* Condylonasal length (mm): less than 78 (0); 78–111 (1); 111–160 (2); over 160 (3).

(2) Relative position of infraorbital foramen versus anterior border of the lacrimal: infraorbital foramen anterior (0); both at same position or infraorbital foramen posterior (1).

(3) Dorsal contour of the rostrum in lateral view: nearly straight (0); sigmoid (1).

(4)* Length of upper tooth row (with all molariforms erupted) in relation to the maxillary length at ventral midsagittal line: less than 60% (0); 60–70% (1); over 70% (2).

(5)* Posterior palatal border: long and narrow (0); long and broad (1); short and broad to straight (2).

(6) Posterior palatal angle (measured between the posteriormost point of the interpalatine suture and the posteriormost medial free border of the palate): less than 80° (0); over 80° (1).

(7) Posterolateral border of palate strongly keeled: absent (0); present (1).

(8) Condition of palatine: with longitudinal wrinkle and lateral narrowing (0); completely flat (1).

(9)* Length of infraorbital canal in relation to anteroposterior dimension of lacrimal: less than 40% (0); 40–60% (1); over 60% (2).

(10) Width of temporal fossa in relation to cranial width at the level of the frontoparietal suture: less than 9% (0); 9% and over (1).

(11) Foramina in principal sulcus of buckler osteoderms: restricted to cranial half (0); all over the sulcus (1).

(12) Remarkably large foramina in principal sulcus of buckler osteoderms: absent (0); present (1).

(13) Number of foramina in the principal sulcus of buckler osteoderms: never more than 5 (0); at least some osteoderms with more than 5 (1).

(14) Foramina in the principal sulcus of buckler osteoderms: never in the intersection with the radial sulcus (0); at least some osteoderms with one or more foramina in the intersection with the radial sulcus (1).

(15) Principal sulci in ornamented portion of movable osteoderms: anteriorly free in all osteoderms (0); anteriorly connected in some osteoderms (1).

(16) Foramina anterior to principal sulcus/sulci in ornamented portion of movable osteoderms: absent (0); present in at least some osteoderms (1).

(17)* Total number of foramina in the principal sulcus/sulci of movable osteoderms: never more than 5 (0); 5–13 (1); at least some osteoderms with more than 13 (2).

(18) Number of piliferous foramina in the posterior border of movable osteoderms: never more than 3 (0); at least some osteoderms with 4 or more (1).

APPENDIX 3. Character-taxon matrix used in the cladistic analysis. n/a, not applicable data; —, missing data.

	1	2	3	4	5	6	7	8	9	10	11	12	13	14	15	16	17	18
Stegotherium tauberi	2	0	0	—	0	—	0	0	0	0	n/a	n/a	n/a	n/a	n/a	n/a	n/a	1
Anadasypus hondanus	—	—	—	—	—	—	—	—	—	—	0	0	0	1	0	1	1	0
Dasypus punctatus	2	0	1	2	1	0	1	1	—	—	1	0	1	1	1	1	2	1
Dasypus hybridus	0	1	0	1	0	0	0	0	1	1	1	0	1	1	1	1	1	1
Dasypus kappleri	2	1	1	0	2	1	1	1	1	1	1	0	1	1	1	—	1	1
Dasypus novemcinctus	1	1	1	1	2	1	0	0	1	1	1	0	1	1	1	1	1	1
Dasypus septemcinctus	0	1	0	1	—	—	0	0	2	1	—	0	—	1	—	—	—	1
Propraopus grandis	3	0	—	—	1	0	0	0	0	0	0	1	0	0	0	0	0	0
Propraopus sulcatus	—	—	—	—	—	—	—	—	—	—	0	1	0	0	0	0	1	0